

Mechanism of Thermal Unimolecular Decomposition of TNT (2,4,6-Trinitrotoluene): A DFT Study

Revital Cohen,[†] Yehuda Zeiri,[‡] Elhanan Wurzberg,[§] and Ronnie Kosloff^{*,||}

Chemical Research Support Unit, Department of Chemistry, Weizmann Institute of Science, Rehovot, 76100, Israel, Chemistry Department, NRCN, P.O. Box 9001, Beer-Sheva 84190, Israel, Rafael Intelligence and Security Directorate, P.O. Box 2250, Haifa, 31021, Israel, and Fritz Haber Center for Molecular Dynamics, Hebrew University, Jerusalem 91904, Israel

Received: March 16, 2007; In Final Form: June 15, 2007

The widespread and long-term use of TNT has led to extensive study of its thermal and explosive properties. Although much research on the thermolysis of TNT and polynitro organic compounds has been undertaken, the kinetics and mechanism of the initiation and propagation reactions and their dependence on the temperature and pressure are unclear. Here, we report a comprehensive computational DFT investigation of the unimolecular adiabatic (thermal) decomposition of TNT. On the basis of previous experimental observations, we have postulated three possible pathways for TNT decomposition, keeping the aromatic ring intact, and calculated them at room temperature (298 K), 800, 900, 1500, 1700, and 2000 K and at the detonation temperature of 3500 K. Our calculations suggest that at relatively low temperatures, reaction of the methyl substituent on the ring (C–H α attack), leading to the formation of 2,4-dinitro-anthranil, is both kinetically and thermodynamically the most favorable pathway, while homolysis of the C–NO₂ bond is endergonic and kinetically less favorable. At \sim 1250–1500 K, the situation changes, and the C–NO₂ homolysis pathway dominates TNT decomposition. Rearrangement of the NO₂ moiety to ONO followed by O–NO homolysis is a thermodynamically more favorable pathway than the C–NO₂ homolysis pathway at room temperature and is the most exergonic pathway at high temperatures; however, at all temperatures, the C–NO₂ \rightarrow C–ONO rearrangement–homolysis pathway is kinetically unfavorable as compared to the other two pathways. The computational temperature analysis we have performed sheds light on the pathway that might lead to a TNT explosion and on the temperature in which it becomes exergonic. The results appear to correlate closely with the experimentally derived shock wave detonation time (100–200 fs) for which only the C–NO₂ homolysis pathway is kinetically accessible.

Introduction

2,4,6-Trinitrotoluene (TNT) has been available as a pure material since 1870. At present, TNT is a major military explosive despite the development of more potent alternatives. TNT is cheap and safe, it is easy to prepare, and it has a low hygroscopicity, relatively low sensitivity to impact and friction, good thermal stability, and relatively high power during detonation. The widespread and long-term use of TNT has led to extensive study of its thermal and explosive properties.^{1–9} Considerable evidence exists that the thermal decomposition processes of TNT and other explosives are related to their sensitivity to impact and shock energy.¹ Consequently, thermal decomposition chemistry is fundamentally important in the explosives field,^{10,11} and the determination of the kinetics and mechanism of the thermal decomposition of TNT remains a fundamental aspect of its characterization.

There is substantial evidence that one or more of the following initiation steps take place during the thermolysis of polynitro compounds: (1) C–NO₂ homolysis, (2) isomerization of the

nitro (NO₂) group to the nitrite (ONO), and (3) reactions of the nonenergetic substituent on the ring (CH₃ in the case of TNT).^{1,3} The relative importance of these initiation steps depends on the reaction conditions (temperature and pressure). Currently, it is believed that at lower temperatures (<800–900 °C), the initiation chemistry of TNT is dominated by oxidation reactions of the methyl group and that at elevated temperatures (>800–900 °C), C–NO₂ homolysis dominates the initiation process.² However, there is no direct evidence for the latter occurrence but rather circumstantial indications for the formation of an aromatic radical.⁹ NO₂(g) was rarely detected as a decomposition product; however, large quantities of NO(g) have been observed.^{12,13} Knowledge about aromatic -NO₂ to -ONO rearrangement is deficient, although nitro–nitrite isomerization has been shown to take place in nitrobenzene derivatives containing donor substituents.^{3,14} Decomposition of the nitrite is a plausible source of the large amount of NO(g) that is generated by many polynitrobenzene derivatives upon rapid thermal decomposition.^{1,3,14} Unlike nitro aliphatic compounds, where the nitrite isomer of the respective nitro compound has been isolated, no aryl nitrite compound has been isolated to date. This might suggest that if and when formed, aromatic nitrite rapidly decomposes to form NO(g) and an oxygen radical. Indirect evidence for the formation of the latter exists but is relatively scarce.^{3,9,14}

* Corresponding author. E-mail: ronnie@fh.huji.ac.il; fax: 972-2-6513742.

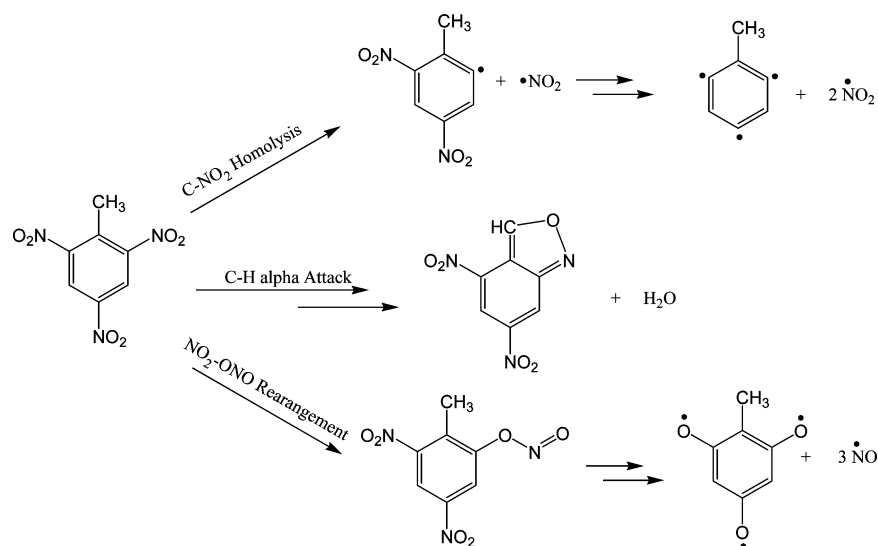
[†] Weizmann Institute of Science.

[‡] NRCN.

[§] Rafael Intelligence and Security Directorate.

^{||} Hebrew University.

SCHEME 1



Although much research on the thermolysis of TNT and polynitro organic compounds has been undertaken, the kinetics and mechanism of the initiation and propagation reactions and their dependence on the temperature and pressure are unclear. To understand the explosive nature of TNT, the kinetics and mechanism of its thermal decomposition need to be examined in detail to clarify its detonation mechanism. Very few theoretical studies have been reported for TNT or other nitro aromatic compounds.^{8,15–17} We have previously reported a computational study on the thermal decomposition leading to detonation of triacetoneperoxide (TATP).^{10,11} Calculations related to TNT decomposition are limited to small model systems^{8,15–17} and to relatively low levels of theory.^{8,15} We are not aware of any comprehensive thermochemical DFT analysis of TNT decomposition.

It is precarious to equate the findings of unimolecular chemistry in the gas phase directly to the reactions in the condensed phase. Nevertheless, we suggest that the first steps of the reaction schemes induced by heat, light, and ionizing radiation in different phases of nitro aromatic compounds are similar. We therefore exclude further oxidation by atmospheric oxygen. The rationale is a separation of time scales between the reactions that take place on the time scale of detonation wave propagation and subsequent secondary reactions that further degrade the parent molecule. Computational investigation of the mechanisms that are involved in the thermal decomposition of a single TNT molecule will therefore shed light on the chemical processes that are involved in its detonation.

Here, we report a comprehensive computational DFT investigation of the unimolecular adiabatic (thermal) decomposition of TNT. It is conceivable that during TNT detonation, a large portion of it decomposes to water, CO, and CO₂ as final products supplying the main energy release. These products are formed in a second stage of reactions that occur after the detonation shock wave passes. In our investigation, we concentrated on the processes that led to the explosion rather than on the processes that took place during and after it. Moreover, such reactions may involve atmospheric species as well as nearby radicals and first stage detonation products. Exploring these reaction mechanisms is beyond the scope of this paper. It has been shown that aromatic ring fission does not take place until most of the attached substituents are removed.^{1,4} We believe that ring fission is a process that most probably takes place during TNT detonation and not the process that leads to it as

the C–C bond dissociation energy (BDE) (~100–150 kcal/mol), especially in aromatic rings, is much larger than the C–N (~70 kcal/mol), O–N (~50 kcal/mol), or C–H (~100 kcal/mol) BDEs; the dissociation of these bonds occurs at the initial stages (and usually the rate determining state (RDS)) of the decomposition pathways considered here (vide infra).¹⁸ Thus, we concentrate our investigation on the kinetics and mechanism of the processes that take place before the aromatic ring is dissociated.

In our investigation, TNT decomposition is assumed to be unimolecular. We base our assumption on the experimental evidence that the detonation rate of TNT is ~ 6900 m/s and that the size of the TNT unit cell in the bulk is roughly 10–20 Å.^{19–21} Accordingly, the time it takes the shock wave generated by the initial detonation to cross approximately one unit cell is roughly 150–300 fs. This time scale is probably too short to allow bimolecular reactions (followed, i.e., by radical formation) that will cause the explosion. Such reactions were shown to take place during millisecond time scales.² Thus, detonation of TNT is a result of a unimolecular decomposition rather than of intermolecular radical chain propagation reactions.²² It is inferred that the detonation of TNT and similar molecules is caused by a rapid release of work accompanied by an abrupt increase in the pressure due to a fast increase in the number of decomposition products. Following this inference, we investigated three decomposition routes that led to detonation;²³ their initial steps were previously proposed to have contributed to TNT decomposition initiation.¹ Two of our proposed mechanisms result in the evolution of four gas molecules out of one bulk molecule. All the investigated routes are described in Scheme 1.

In the first route, C–NO₂ homolytic cleavage takes place followed by subsequent C–NO₂ homolysis steps forming eventually three NO₂(g) molecules and an aromatic triradical intermediate. In the second route, C–H attack on the nitro substituent takes place to form 2,4-dinitro-anthranil (DNAn) and water, and in the third route, nitro–nitrite (C–NO₂ → C–ONO) rearrangement takes place followed by O–NO homolytic cleavage and the release of NO(g) for each of the three NO₂ substituents.²³

There is indirect experimental evidence for the initial step of the first route (C–NO₂ homolysis)^{1,9,13} and for the second route^{2,6,7} to occur in the thermal decomposition of TNT, while for the third route, the only indirect evidence found so far is the release of large quantities of NO(g) in a few experiments

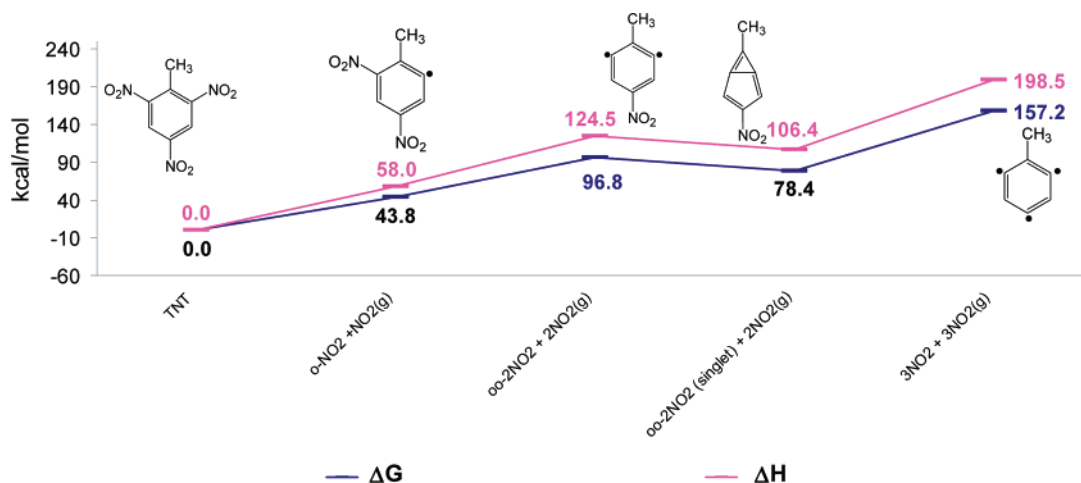


Figure 1. Enthalpy and free energy plots for C–NO₂ homolysis pathway as calculated at the uB3LYP/cc-pVDZ level of theory.

and the formation of a phenolic radical.^{1,12,13} We have calculated the free energy pathways for these three routes using the Gaussian 03²⁴ program package in the uB3LYP^{25,26}/cc-pVDZ²⁷ level of theory. We took into account the thermal corrections to the relative energies of the intermediate and transition states both at room temperature (298 K) and at elevated temperatures, including the estimated detonation temperature of 3500 K generated during TNT explosion. On the basis of the temperature analysis, we attempted to estimate the most favorable pathway that leads to TNT detonation and the temperature range for which it becomes dominant. The temperature analysis was carried out to obtain general guidance for the difference between the thermal decomposition at room temperature and the thermal decomposition at higher temperatures. The analysis is aimed at qualitative identification of the process that takes place during the initiation stage eventually leading to detonation.

Computational Methods

All calculations were carried out using DFT as implemented in the Gaussian 03 program.²⁴ The Becke three-parameter hybrid density functional method with the Lee–Yang–Parr correlation functional approximation (B3LYP)^{25,26} was employed together with the Dunning correlation-consistent polarized valence double- ζ (cc-pVDZ) basis set.²⁷ This level of theory was shown to be adequate for calculating the detonation mechanism of similar sized systems.¹⁰

The structures that had an open shell character were located using the unrestricted uB3LYP method wave function. This spin-unrestricted approach has been demonstrated to describe correctly diradical intermediates as well as transition states when multireference problems are present.²⁸ Geometry optimizations for minima were carried out using the standard Berny algorithm^{29,30} in redundant internal coordinates up to the neighborhood of the solution and, then, if not converged, continued the optimization using analytical second derivatives.³¹ Optimizations for transition states were carried out with an initial guess for the transition state being generated from manual manipulation of the geometry using MOLDEN.³² In cases where this approach failed to converge, we used analytical second derivatives at every step.

Zero-point and RRHO (rigid rotor-harmonic oscillator) thermal corrections (to obtain ΔS and ΔG values) were obtained from the unscaled computed frequencies both for room temperature (298 K) and for higher temperatures (800, 900, 1500, 1700, 2000, and 3500 K).

Results and Discussion

Thermal Decomposition of TNT at Ambient Temperature

C–NO₂ Homolysis. The C–NO₂ bond is usually the weakest bond of nitro aromatic compounds. It was experimentally suggested that C–NO₂ homolysis is the dominant initial reaction that takes place in the decomposition channel of 3- and 4-nitrotoluene and also occurs for 2-nitrotoluene.¹ In the gas phase, it was proposed that this reaction competes with two other reactions (NO₂ isomerization and C–H α attack, see following description).³³ Nevertheless, C–NO₂ homolysis is most probably the favored decomposition channel of nitro aromatic compounds in the gas phase at high temperatures.¹ We have calculated a pathway that is initiated by C–NO₂ homolysis followed by subsequent C–NO₂ homolysis of the two remaining substituents of TNT since C–NO₂ is the weakest bond of TNT, and it has been shown that aromatic ring fission does not take place until most of the attached substituents are removed.¹⁴ This is the most straightforward way to generate four gas molecules out of one. The enthalpy and free energy pathway for the homolytic cleavage of all three nitro substituents in TNT is presented in Figure 1. The increasing contribution of entropy to the ΔG energy is indicated by the increasing energy differences between the ΔG and the ΔH pathways as more NO₂ molecules are being eliminated.

According to our calculations during the first step of C–NO₂ homolytic cleavage in TNT, the ortho NO₂ is eliminated, and an aromatic radical and NO₂(g) are formed with $\Delta G = 43.8$ kcal/mol ($\Delta H = 58$ kcal/mol). This value is consistent with the activation energy value of 40.9 kcal/mol that was assigned for NO₂ removal in an early radical producing step obtained by EPR studies.³⁴ It also resembles the value obtained by semiempirical calculations of C–NO₂ homolysis.¹⁵ The ΔG value for initial cleavage of the *para*-NO₂ substituent was found to be 8 kcal/mol higher in energy than for *o*-NO₂; thus, it is less likely to be cleaved initially.

The pathway continues with the homolysis of the two remaining C–NO₂ bonds, which are the weakest bonds in TNT. The energy invested in the cleavage of the second *o*-C–NO₂ bond was found to be $\Delta G = 53.1$ kcal/mol ($\Delta H = 66.5$ kcal/mol), 3.2 kcal/mol lower in energy than the energy required to cleave the *p*-C–NO₂ bond; thus, it is conceivable that *o*-NO₂ will be eliminated preferentially. The homolysis energy of the third *p*-C–NO₂ bond was calculated as $\Delta G = 60.4$ kcal/mol ($\Delta H = 74$ kcal/mol). We could not locate the transition state for C–NO₂ homolysis. However, it should be noted that normally radical recombination, which is the microscopic

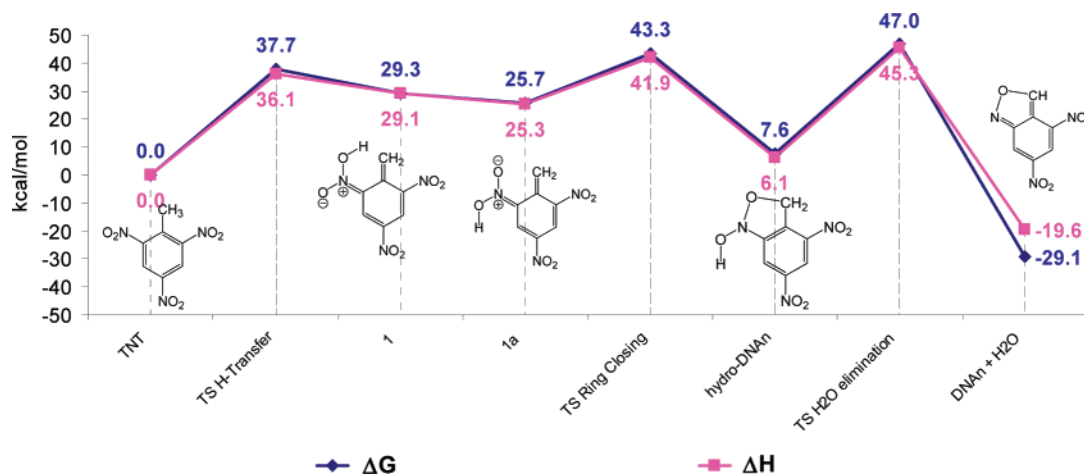


Figure 2. Enthalpy and free energy plots for the C–H α attack pathway as calculated at the uB3LYP/cc-pVDZ level of theory.

reversible reaction of homolysis, takes place without an activation barrier.³⁵ In this case, the observed activation energy for a bond dissociation process is equal to the bond dissociation energy ($\text{BDE}_{\text{C}-\text{NO}_2}$).³⁶ Accordingly, the barrier height for C–NO₂ homolysis is expected to be equal or similar to its BDE (43.8 kcal/mol for the first NO₂, 53.1 kcal/mol for the second, and 60.4 kcal/mol for the third), as reported for N–NO₂ homolysis.^{35,37,38} The closed shell singlet spin derivative of *o,o*-2NO₂ was found to be 18.5 kcal/mol energetically more stable than the *o,o*-NO₂ diradical (triplet); thus, it could be formed as an intermediate (instead of the *o,o*-2NO₂ diradical) before the third C–NO₂ homolysis takes place.

Figure 1 shows that at room temperature, the calculated C–NO₂ homolysis pathway of TNT is both kinetically and thermodynamically unfavorable since every step in the pathway is endergonic. However, the calculated ΔS associated with each C–NO₂ homolysis step is positive, and its values are between 44 and 48 eu, which are relatively large. Since the entropy of C–NO₂ homolysis is positive, its contribution to the ΔG value as the temperature increases will rise according to $\Delta G = \Delta H - T\Delta S$. As a result, at elevated temperatures, the overall ΔG for the pathway will decrease, and the pathway will be less endergonic.

C–H α Attack To Form 2,4-DNAn. NO₂(g) was observed from decomposition of nitro aromatic compounds in the gas phase but was rarely detected in the decomposition of these molecules in the bulk state. This is in contrast to aliphatic nitro compounds in which NO₂(g) is always detected during their decomposition.¹ These observations suggest that nitro aromatic compounds may have alternate decomposition channels whose activation energies lie below that of C–NO₂ homolysis, especially when other substituents are present on the ring. There is considerable evidence for the formation of anthranil and its derivatives in the slow thermal decomposition of nitro aromatic compounds.^{1,2,4,6,7,33,39} The mechanism of DNAn formation was studied in several nitro aromatic compounds, and it was suggested that intramolecular hydrogen transfer from the methyl substituent to the NO₂ moiety is the RDS of the reaction.^{15,17,39} We have calculated the enthalpy and free energy pathway for the formation of 2,4-DNAn from TNT decomposition. The pathway is presented in Figure 2. Since the entropy contribution to the C–H α attack pathway is negligible (until the last water elimination step), the free energy values are very similar to the enthalpy values along the whole pathway.

In the first step of the C–H α attack mechanism, the hydrogen atom is transferred from the toluene CH₃ group to the *o*-nitro substituent in a concerted (one step) mechanism (tautomeriza-

tion). The calculated barrier height for the tautomerization is 37.7 kcal/mol, and the transition state that leads to the formation of tautomer **1** is an ordered six-membered ring with the methyl hydrogen positioned between the methyl carbon and the NO₂ oxygen in distances of 1.483 and 1.155 Å, respectively (Figure 3).

In the second step, there is a rotation around the C=N bond, generating the more stable (by 3.6 kcal/mol) tautomer **1a** with the oxygen atom positioned in close proximity to the methylene group. The next step is ring closure by an attack of the HONO oxygen on the methylene carbon to form the five-membered ring of the hydro-DNAn with a calculated $\Delta G^\ddagger = 17.6$ kcal/mol for the transition. The last step, which makes the overall pathway exergonic and thus thermodynamically favorable, is the elimination of a water molecule by hydroxyl attack on the methylene hydrogen and formation of the rigid heterocyclic DNAn, which is 29.1 kcal/mol more stable than TNT. The barrier height for water elimination is 39.4 kcal/mol, which according to our calculations is also the RDS of the reaction. This is in contrast to previous reports claiming that the hydrogen transfer step is the RDS of the reaction.⁴⁰ It should be noted, however, that previous observations were based on a primary H/D isotope effect, suggesting that C–H bond scission is involved in the RDS.⁴⁰ Elimination of a water molecule also involves C–H bond scission, and thus, our calculations are supported by experimental evidence.

The C–H α attack pathway is exergonic at room temperature, unlike the endergonic C–NO₂ homolysis pathway, and it is also kinetically more favorable (as the RDS is lower in energy than the initial C–NO₂ homolysis step). Thus, at mild temperatures,

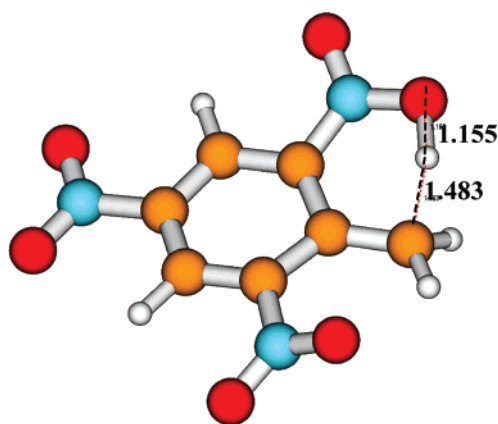


Figure 3. TS for H-transfer in the C–H α attack pathway.

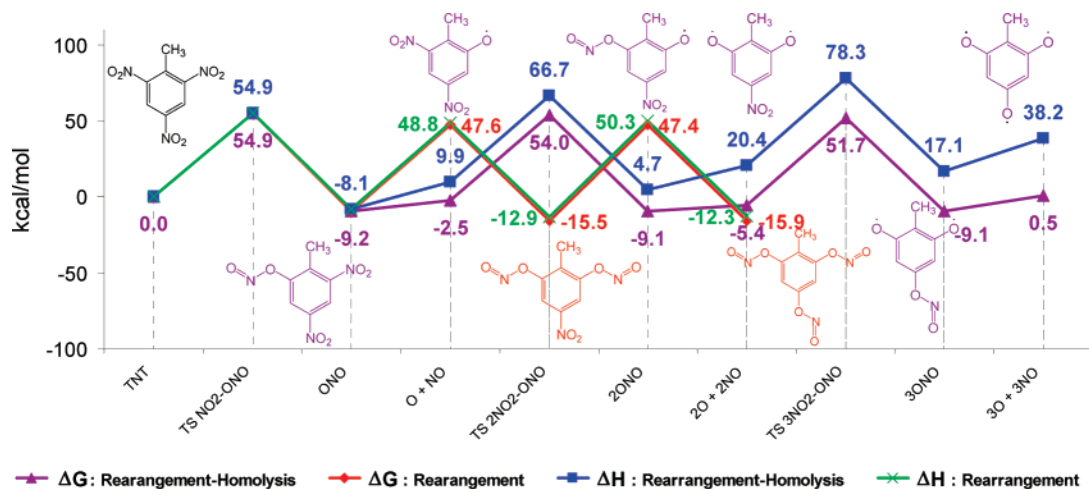


Figure 4. Enthalpy and free energy plots for the C-NO₂ → C-ONO rearrangement and C-NO₂ → C-ONO rearrangement-homolysis pathways as calculated at the uB3LYP/cc-pVDZ level of theory.

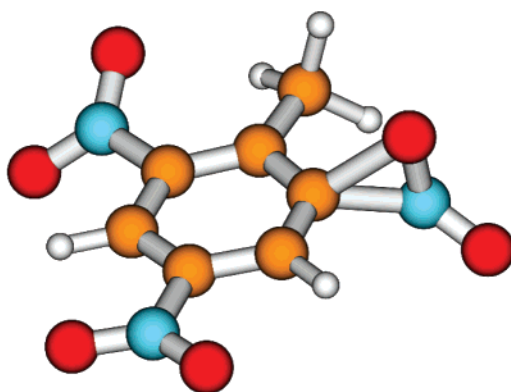


Figure 5. TS for NO₂ to ONO rearrangement.

it is more likely to take place than the C-NO₂ homolysis pathway. However, as the temperature increases, the ordered transition states for hydrogen transfer ($\Delta S^\ddagger = -5.4$ eu), ring formation ($\Delta S^\ddagger = -4.6$ eu), and water elimination ($\Delta S^\ddagger = -5.7$ eu) processes are expected to increase in energy due to the increased contribution of the entropy term ($T\Delta S$) to ΔG . Thus, at elevated temperatures, the C-H α attack pathway might become kinetically unfavorable.

C-NO₂ → C-ONO Rearrangement-Homolysis. Experimental evidence suggest that C-NO₂ homolysis in the gas phase, is a major early thermal decomposition reaction of nitro aromatic compounds at high temperatures; however, the role of this channel as compared to C-NO₂ isomerization is difficult to assess in the condensed phase. NO₂(g) was rarely detected as a decomposition product in experimental studies of the thermal decomposition of TNT.¹ However, the evolution of large quantities of NO(g) has been reported in a few studies.^{12,13} Nitro-nitrite isomerization is known to take place in aliphatic nitro compounds⁴¹ and has been shown to take place in nitrobenzene derivatives containing electron donating substituents.^{3,14} Decomposition of the nitrite is a plausible source of the large amount of NO(g) generated upon rapid thermal decomposition of nitro aromatic compounds. In the condensed phase, or under increased pressure, isomerization could be important because of TNT's low volume of activation.

We have calculated the pathway for nitro-nitrite isomerization and decomposition of the nitrite as a possible pathway for the decomposition of TNT and the generation of three molecules of NO(g). The pathway is described in Figure 4.

Figure 4 describes the C-NO₂ → C-ONO rearrangement pathway and the C-NO₂ → C-ONO rearrangement-homolysis pathway. Since entropy contributions to the C-NO₂ → C-ONO rearrangement pathway are negligible, the free energy values are very similar to the enthalpy values along the pathway. However, in the C-NO₂ → C-ONO rearrangement-homolysis pathway, the increasing contribution of entropy to the ΔG energy is indicated by the increasing energy differences between the ΔG and the ΔH pathways as more NO molecules are being eliminated.

In the first step of both pathways, the *o*-NO₂ substituent isomerizes to its nitrite (ONO) derivative. This step is mildly exergonic ($\Delta G = -9.2$ kcal/mol); however, the barrier height ($\Delta G^\ddagger = 54.9$ kcal/mol) for the rearrangement at room temperature is relatively high (which makes this step the RDS of the pathway), suggesting that this step is kinetically unfavorable at room temperature. It should be noted that the experimentally estimated activation energy for C-NO₂ → C-ONO rearrangement in nitro aromatic compounds is 56 kcal/mol, which closely resembles our calculated barrier for the transition. The transition state (TS) structure for C-NO₂ → C-ONO rearrangement is an ordered TS in which both the O and the N atoms are positioned in close proximity to the aromatic carbon (Figure 5).

The next step is O-NO homolysis. The energy required to cleave the O-NO bond is only 6.7 kcal/mol, and the products O and NO(g) are slightly more stable than TNT, which makes the formation of O and NO(g) thermodynamically favorable. We have not found the TS for O-NO homolysis; however, we expect this reaction to be barrierless as the microscopic reversible reaction (the recombination of radicals) is mostly regarded to be barrierless. If a barrier exists for O-NO homolysis, it is expected to be significantly lower than for the previous rearrangement step. Thus, most probably as soon as the nitrite derivative of TNT is formed, O-NO cleavage will take place. This postulation is also supported by the fact that no aromatic nitrite was isolated to date; however, the formation of a phenolic radical and NO(g) was observed in a few experiments.¹

The pathway continues with two sequences of NO₂ isomerization and O-NO homolysis to form eventually 3O and 3NO(g). The overall process at 298 K of C-NO₂ → C-ONO rearrangement followed by O-NO homolysis is roughly isoenergetic with TNT. However, the intermediates O and 2O as well as their rearranged derivatives 2ONO and 3ONO are somewhat

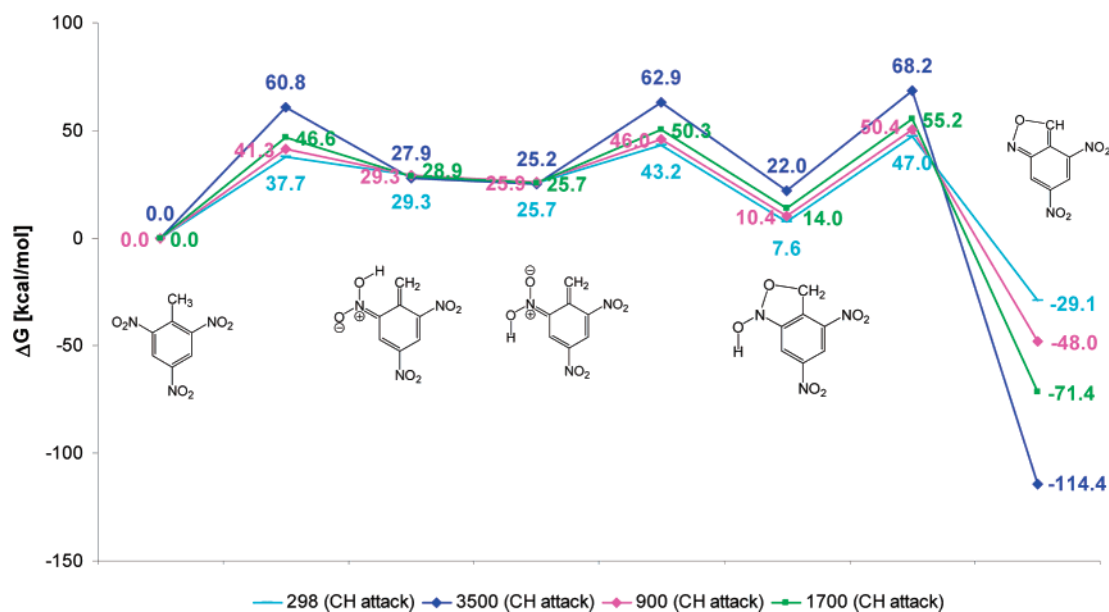


Figure 6. Free energy plots at 298, 900, 1700, and 3500 K for the C–H α attack pathway as calculated at the B3LYP/cc-pVDZ level of theory.

more stable than TNT. We have also calculated the pathway for $\text{C-NO}_2 \rightarrow \text{C-ONO}$ rearrangement without subsequent O-NO homolysis for all three substituents and found it to be slightly more exergonic than the rearrangement-homolysis pathway. However, since the barrier for $\text{C-NO}_2 \rightarrow \text{C-ONO}$ isomerization is significantly higher than the one for O-NO homolysis, the rearrangement pathway is kinetically unfavorable. The sequential $\text{C-NO}_2 \rightarrow \text{C-ONO}$ rearrangement-homolysis pathway leads to the formation of four molecules out of one: three of them are of nitric oxide (NO(g)), which is a very stable gas molecule. The associated entropy gain for each O-NO homolysis step is calculated as $\Delta S = \sim 40$ eu, and this relatively large entropy gain is expected to contribute significantly to the ΔG value at elevated temperatures, which might cause this pathway to become thermodynamically favorable. In addition, the formation of four gas molecules from one molecule in the bulk phase can boost the pressure abruptly, which might lead to a TNT explosion. However, the RDS of this pathway is not O-NO homolysis but rather a NO_2 rearrangement that has a negative entropy. At elevated temperatures, the negative entropy term will increase the free energy for this step, causing it to be less kinetically favorable; thus, as the temperature increases, the $\text{C-NO}_2 \rightarrow \text{C-ONO}$ rearrangement-homolysis pathway is expected to become exergonic but kinetically unfavorable.

The result of O–NO homolysis is a stable oxygen radical molecule and NO(g). The relative stability of the products of O–NO homolysis can be understood by the exceptional stability of the NO(g) molecule. In addition, while TNT is a highly electron deficient compound due to its three NO₂ substituents, the TNT oxygen radical derivative is more electron-rich. Thus, release of –one to two NO molecules from TNT stabilizes it by increasing the electron density on the ring.

Unlike in the C–NO₂ homolysis pathway, here the singlet equivalent of 2O (not shown) is higher in energy by 26 kcal/mol than the triplet diradical (2O), and thus, it is unlikely that it will be formed. In this pathway, as in the C–NO₂ homolysis pathway, the ortho substituents are easier to cleave than the para substituents as the para cleaved NO (*p*-O, not shown) and *p,o*-2O (not shown) are 7 and 6.5 kcal/mol higher in energy than *o*-O and *o,o*-2O, respectively.

On the basis of room temperature analysis, it appears that the most favorable pathway, both kinetically and thermody-

namically, is the C-H α attack, which has both the lowest kinetic RDS barrier and is the most exergonic pathway.⁴² The C-NO₂ homolysis pathway is endergonic and, thus, will not occur. The C-NO₂ \rightarrow C-ONO rearrangement-homolysis pathway is isoenergetic with TNT; however, its RDS barrier is larger than the C-H α attack and, thus, will be slower than C-H α and less favorable.

Thermal Decomposition of TNT at Elevated Temperatures. The situation is expected to change at elevated temperatures in which the entropy contributes significantly to ΔG . Since $\Delta G = \Delta H - T\Delta S$, as T increases, the contribution of the second term, $T\Delta S$, becomes greater. In this case, pathways that involve a significant increase in entropy, such as C–NO₂ homolysis and O–NO homolysis, are expected to become more energetically favorable. Pathways that involve a decreased entropy of products and in TS, such as C–H α attack, are expected to be less favorable. The C–NO₂ \rightarrow C–ONO rearrangement–homolysis pathway involves both reduction in the entropy of the C–NO₂ \rightarrow C–ONO rearrangement TS and an increase in the entropy of the products of O–NO homolysis. Although it is expected to be more thermodynamically favorable, it will be less kinetically favorable due to the constrained geometry of the rearrangement transition states. We have conducted a thermochemical analysis of the calculated processes at 3500 K, which is the estimated temperature of the shock wave generated during TNT detonation, and at two additional intermediate temperatures to verify our assumptions. Using the freqchk option of the Gaussian 03 program, we obtained thermal corrections to the Gibbs free energy at 900, 1700, and 3500 K (based on the RRHO approximation). The results of this analysis are presented in Figures 6–8. Since the enthalpy (ΔH) dependence on temperature is negligible, the figures only describe the free energy pathways (ΔG).

As expected, at elevated temperatures, all pathways become more exergonic. The C-NO₂ → C-ONO pathway is the most exergonic, and the C-H α attack is the least exergonic one. However, kinetically, the situation is different. Figure 6 shows that for the C-H α attack pathway, although the overall path becomes more exergonic with increasing the temperature, its TS significantly increases in energy (i.e., from 37.7 kcal/mol at room temperature to 60.8 kcal/mol at 3500 K), which makes this pathway the most kinetically unfavorable one at high

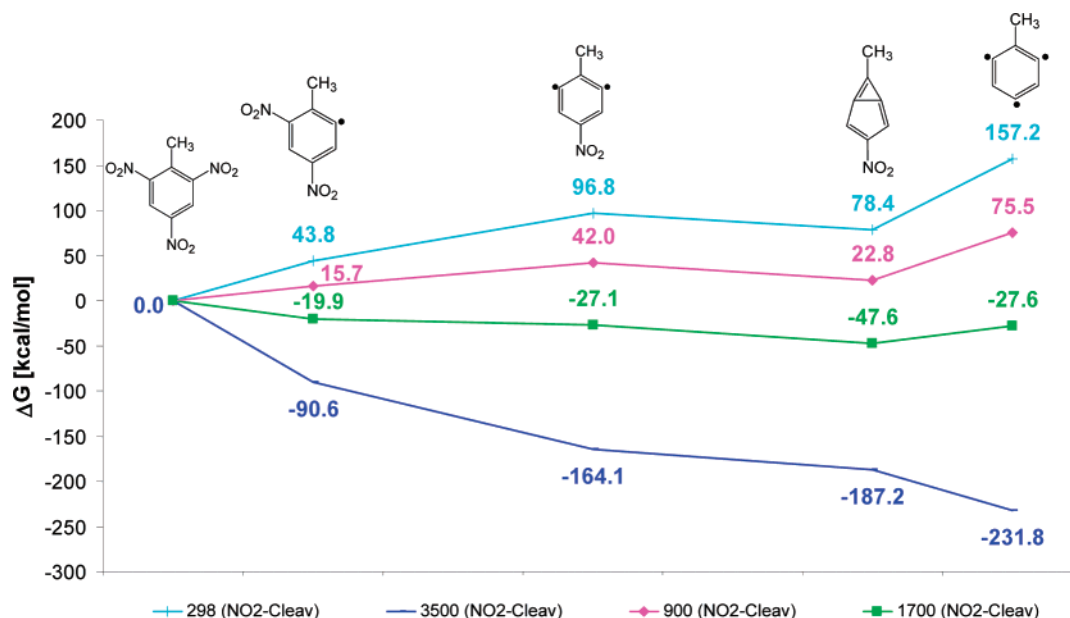


Figure 7. Free energy plots at 298, 900, 1700, and 3500 K for the C-NO₂ homolysis pathway as calculated at the B3LYP/cc-pVDZ level of theory.

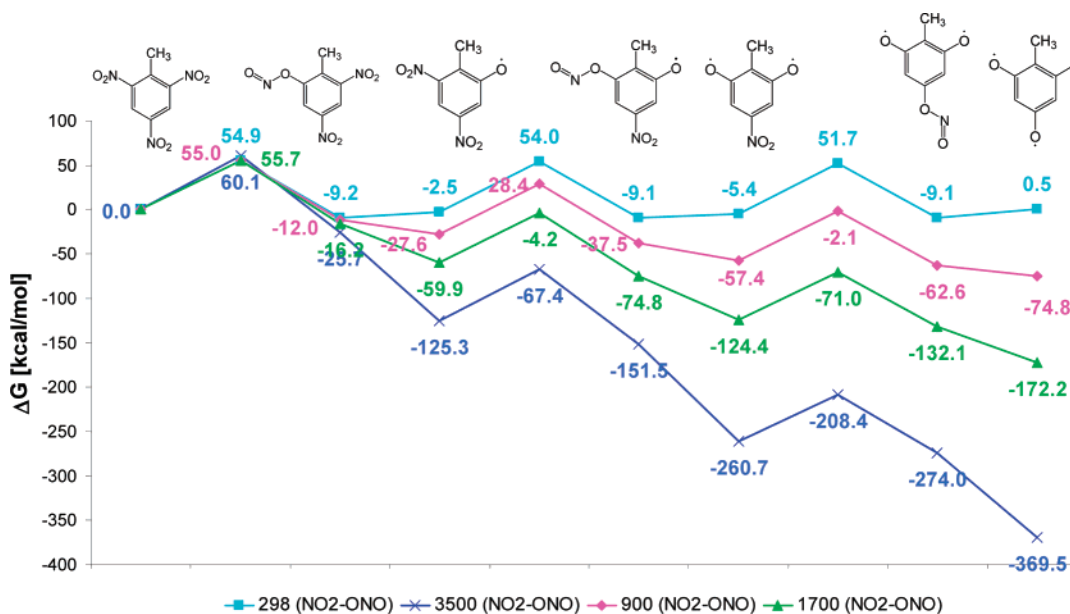


Figure 8. Free energy plots at 298, 900, 1700, and 3500 K for the C-NO₂ → C-ONO rearrangement-homolysis pathway as calculated at the B3LYP/cc-pVDZ level of theory.

temperatures with respect to the other two pathways. In contrast, the C-NO₂ homolysis pathway, although less exergonic than the C-NO₂ → C-ONO pathway, becomes the most kinetically favorable pathway to take place at elevated temperatures as the barrier to cleave the C-NO₂ bond diminishes with increasing the temperature. It should be noted, however, that at 900 K, this pathway is still endergonic and thus is not expected to generate significant heat and to lead to a detonation at this temperature. At 1700 K, it becomes moderately exergonic and kinetically favorable; thus, most probably it is the major decomposition pathway of TNT at this temperature.

The C-NO₂ → C-ONO rearrangement-homolysis pathway becomes the most exergonic pathway at elevated temperatures. However, the first rearrangement step, which is also the RDS of this pathway, is entropically unfavorable; therefore, this pathway becomes less kinetically favorable than the C-NO₂ homolysis.

Comparing the C-NO₂ → C-ONO rearrangement-homolysis and the C-H α attack pathways, it should be noted that although the RDS step of the former is entropically unfavorable, its activation energy rises only slightly with temperature, whereas in the C-H α attack pathway, the activation energy rise with the temperature is more significant. Accordingly, the C-NO₂ → C-ONO rearrangement-homolysis pathway becomes kinetically more favorable than the C-H α attack pathway at temperatures as high as 3500 K (but less favorable at temperatures lower than ~2000 K). However, at such elevated temperatures, the C-NO₂ homolysis pathway is dominant; thus, the contribution of either the C-H α attack pathway or the C-NO₂ → C-ONO pathway to TNT decomposition at high temperatures is negligible.

Our results at elevated temperatures are supported by experimental evidence showing that at moderate temperatures, the C-H α attack pathway dominates the thermal decomposition

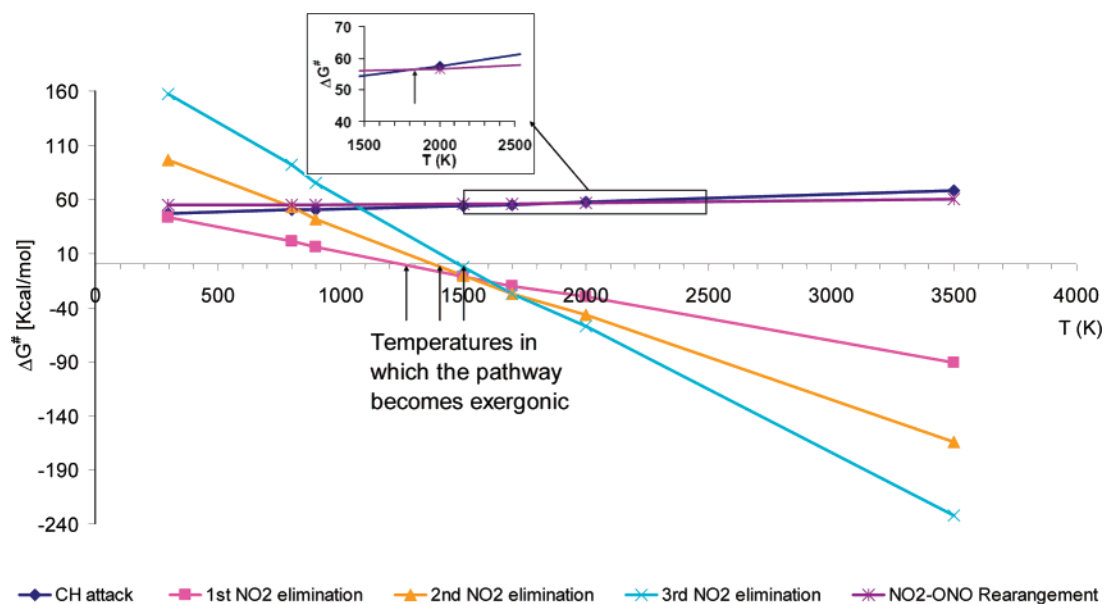


Figure 9. Activation free energy vs temperature for all computed TNT decomposition pathways. Inset illustrates the temperature in which the C-NO₂ → C-ONO rearrangement pathway becomes more kinetically favorable than the CH attack pathway.

of TNT, and at elevated temperatures, C-NO₂ homolysis is the most important pathway. According to our calculations, the most exergonic reaction taking place at 3500 K is the C-NO₂ → C-ONO rearrangement-homolysis. However, it is less favorable kinetically than C-NO₂ homolysis at this temperature and is expected to be slower. We have conducted a kinetic analysis of the relative rates of these two reactions based on the Eyring equation

$$k = \frac{k_B T}{h} e^{-\Delta G^\ddagger/RT} \quad (1)$$

$$t_{1/2} = \frac{\ln 2}{k} \quad (2)$$

where k is the rate, k_B is Boltzmann's constant, h is Planck's constant, ΔG^\ddagger is the RDS free energy barrier, R is the gas constant, T is the temperature in Kelvin, and $t_{1/2}$ is the half-life time in seconds. Implementation of these equations in the present case (where $T = 3500$ K) yields a reactant (TNT) half-life time of 50 ps for the C-NO₂ → C-ONO pathway ($\Delta G^\ddagger = 60$ kcal/mol) and 10 fs for the C-NO₂ pathway ($\Delta G^\ddagger \sim 0$). Since the estimated reaction time during detonation is ~ 150 fs (assuming a shock wave velocity of 6900 m/s during detonation and a typical TNT unit cell size of ~ 10 Å), it appears that although the C-NO₂ → C-ONO pathway is considerably more exergonic than the C-NO₂ pathway and therefore is expected to generate more heat, its relative contribution to detonation is minor since it is 3.5 orders of magnitude slower than the C-NO₂ homolysis reaction.

The situation might be different under extreme pressure, where the C-NO₂ → C-ONO rearrangement might become favorable with respect to C-NO₂ homolysis. If rearrangement takes place to form three ONO derivatives of TNT before C-NO₂ or C-ONO homolysis takes place, then O-NO homolysis ($\Delta G_{\text{O-NO cleavage}}^{298} = 6.7$ kcal/mol) will be favored over C-ONO homolysis ($\Delta G_{\text{C-ONO cleavage}}^{298} = 53$ kcal/mol).

To estimate the temperature range in which the relative importance of the different pathways changes from C-H attack to C-NO₂ homolysis, we have constructed a graph of ΔG^\ddagger versus T for all three pathways (Figure 9). The ΔG^\ddagger value for each pathway is taken as the RDS ΔG^\ddagger value for the specific

temperature. In the case of C-NO₂ homolysis, the pathway was separated into three individual pathways: first, second, and third C-NO₂ eliminations, and for each elimination step, the ΔG^\ddagger value was taken as the ΔG for C-NO₂ cleavage (since the homolysis process was considered to be barrierless). The value for which the ΔG versus T line crossed the X axis (0 kcal/mol) is the temperature in which the pathway becomes exergonic.

Since for NO₂ elimination pathways the ΔG^\ddagger values plotted are the ΔG values for C-NO₂ homolysis, and this event is endergonic at low temperatures, only when ΔG reaches 0.0 kcal/mol does the homolysis pathway become exergonic. Accordingly, Figure 9 shows that the temperatures for which C-NO₂ homolysis becomes exergonic are ~ 1250 K for cleaving one NO₂, ~ 1400 K for two NO₂ groups, and ~ 1500 K for elimination of all three NO₂ groups. Below 1250 K, even if C-NO₂ homolysis takes place (since it has a lower activation energy than the other pathways), it will not generate heat since it is endergonic and might even inhibit the detonation. Thus, at temperatures below 1250 K, the most favorable pathway is the C-H attack since it is exergonic and requires a lower energy than the C-NO₂ → C-ONO rearrangement-homolysis pathway. The temperature in which the C-NO₂ → C-ONO rearrangement-homolysis pathway becomes more favorable than the C-H attack pathway is ~ 1800 K. At this temperature, the C-NO₂ homolysis pathway is already the main decomposition pathway. Thus, before C-NO₂ homolysis begins, the C-H attack pathway is expected to be a major decomposition pathway, whereas C-NO₂ → C-ONO rearrangement-homolysis is expected to have a minor contribution.

To determine which pathway takes place at the estimated detonation time of the TNT detonation shock wave (100–200 fs), we constructed an Arrhenius plot ($\ln k$ vs $1/T$) (Figure 10). The values of $\ln k$ were calculated using the Eyring equation (eq 1) in which the ΔG^\ddagger value for each pathway is assumed to be the RDS ΔG^\ddagger value at the specified temperature. For C-NO₂ homolysis, the decomposition pathway was again separated into three individual paths: first, second, and third C-NO₂ eliminations. For each elimination of an NO₂ group, the ΔG^\ddagger value is assumed to be given by the ΔG value for C-NO₂ cleavage. The $\ln k$ values for detonation with $t_{1/2}$ in the range of 100–200 fs are 29.6–28.9, respectively (eq 2). The pathways that

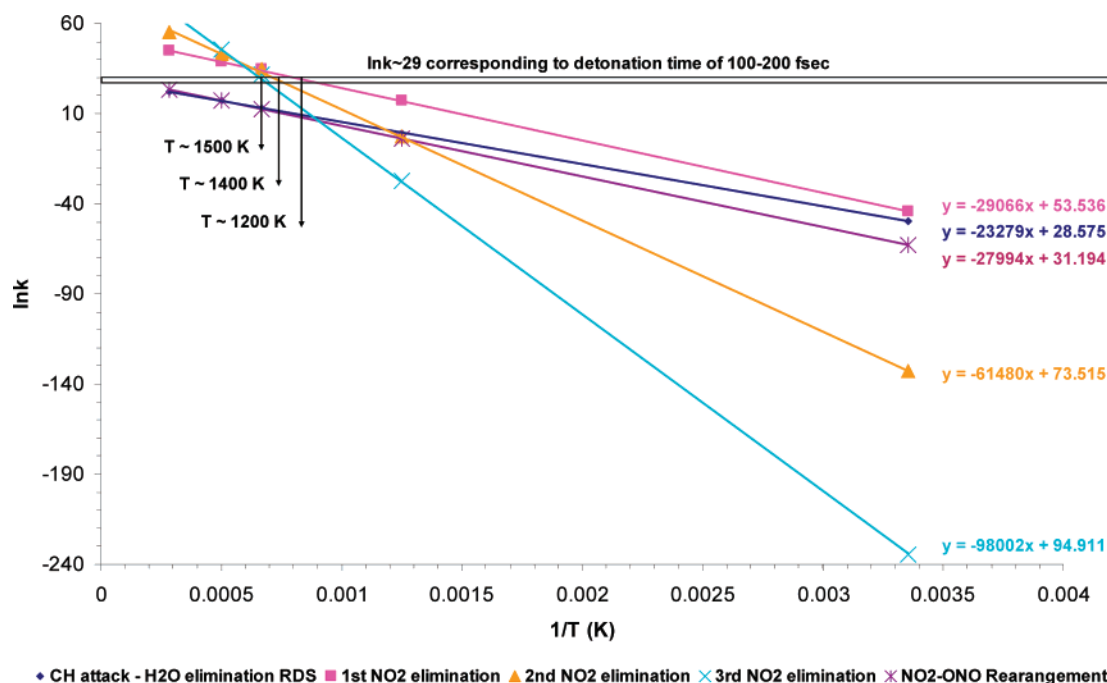


Figure 10. Arrhenius plot ($\ln k$ vs $1/T$) for TNT decomposition pathways. $\ln k$ values are calculated from the Eyring equation (eq 1) in which the ΔG^\ddagger for each pathway is assumed to be the RDS at the specified temperature.

cross the window of these $\ln k$ values represent the pathways that are kinetically accessible during TNT detonation in specific temperatures. According to Figure 10, only three pathways out of the five examined can “cross the window” of $\ln k$ values of 28.0 and 30.0, in the temperature range of 200–4000 K: first, NO_2 elimination at ~ 1200 K; second, NO_2 elimination at ~ 1400 K; and third, NO_2 elimination at ~ 1500 K.

This suggests that for the estimated detonation time scale, only the C– NO_2 homolysis pathway is kinetically accessible. The C–H attack and the C– $\text{NO}_2 \rightarrow$ C–ONO rearrangement–homolysis pathways are too slow to generate a shock wave with a detonation velocity of 6900 m/s and thus are kinetically inaccessible. The results here suggest that the temperature range in which the C– NO_2 homolysis occurs consistently with this time scale is 1200–1500 K. At this temperature range, it was shown that C– NO_2 homolysis becomes exergonic and thus favorable with respect to the other two possible decomposition pathways. Thus, even though TNT decomposition can take place at lower temperatures than 1200 K, it most probably will not lead to detonation before C– NO_2 homolysis becomes exergonic.⁴³

In conclusion, we conducted a computational study of the unimolecular thermal decomposition of TNT to elucidate its explosive nature. On the basis of previous experimental observations, we have postulated three possible pathways for TNT decomposition, keeping the aromatic ring intact, and calculated them at room temperature (298 K), 800, 900, 1500, 1700, 2000, and at the detonation temperature of 3500 K (which is the estimated temperature generated during TNT explosion). Our calculations suggest that at relatively low temperatures, the C–H α attack, leading to the formation of 2,4-DNAn, is both kinetically and thermodynamically the most favorable pathway, while the C– NO_2 homolysis pathway is endergonic and kinetically less favorable. At ~ 1250 –1500 K, the situation changes, and the C– NO_2 homolysis pathway dominates TNT decomposition. C–H α attack becomes both kinetically unfavorable and thermodynamically less favorable as compared to the C– NO_2 homolysis pathway. The C– $\text{NO}_2 \rightarrow$ C–ONO rearrangement–homolysis pathway is thermodynamically more

favorable than C– NO_2 homolysis at room temperature and is the most exergonic pathway at high temperatures; however, at all temperatures, the C– $\text{NO}_2 \rightarrow$ C–ONO rearrangement–homolysis pathway is kinetically unfavorable as compared to the other two pathways and thus is slower. As a result, its contribution to the TNT decomposition is expected to be minor. The computational temperature analysis shed light on the pathway that leads to TNT explosion and on the temperature when the decomposition becomes exergonic. The results appear to correlate closely with the experimental time scale (100–200 fs) derived from the shock wave velocity for which only the C– NO_2 homolysis pathway is kinetically accessible. We are currently performing atomistic scale molecular dynamic simulations^{11,44,45} for initial chemical events in the thermal decomposition of TNT; we have preliminary results that support our DFT calculations.

Acknowledgment. This research was supported by the MAFAT Israel Defense Research Agency. The Fritz Haber Research Center is supported by the Minerva Gesellschaft für die Forschung, GmbH München, FRG.

Supporting Information Available: Full Gaussian 03 citation (ref 24) and XYZ coordinates of all calculated compounds. This material is available free of charge via the Internet at <http://pubs.acs.org>.

References and Notes

- (1) Brill, T. B.; James, K. J. *Chem. Rev.* **1993**, *93*, 2667.
- (2) Brill, T. B.; James, K. J. *J. Phys. Chem.* **1993**, *97*, 8759.
- (3) Brill, T. B.; James, K. J.; Chawla, R.; Nicol, G.; Shukla, A.; Futrell, I. H. *J. Phys. Org. Chem.* **1999**, *12*, 819.
- (4) Singh, G.; Kapoor, I. P. S.; Mannan, S. M.; Tiwari, S. K. *J. Hazard. Mater.* **1999**, *68*, 155.
- (5) Long, G. T.; Brems, B. A.; Wight, C. A. *Thermochim. Acta* **2002**, *388*, 175.
- (6) Dacons, J. C.; Adolph, H. G.; Kamlet, M. J. *J. Phys. Chem.* **1970**, *74*, 3035.
- (7) Rogers, R. N. *Anal. Chem.* **1967**, *39*, 730.
- (8) Dewar, M. J. S.; Ritchie, J. P.; Alster, J. J. *Org. Chem.* **1985**, *50*, 1031.

- (9) Gonzalez, A. C.; Larson, C. W.; Mcmillen, D. F.; Golden, D. M. *J. Phys. Chem.* **1985**, 89, 4809.
- (10) Dubnikova, F.; Kosloff, R.; Almog, J.; Zeiri, Y.; Boese, R.; Itzhaky, H.; Alt, A.; Keinan, E. *J. Am. Chem. Soc.* **2005**, 127, 1146.
- (11) van Duin, A. C. T.; Zeiri, Y.; Dubnikova, F.; Kosloff, R.; Goddard, W. A. *J. Am. Chem. Soc.* **2005**, 127, 11053.
- (12) Hand, C. W.; Merritt, C.; Dipietro, C. *J. Org. Chem.* **1977**, 42, 841.
- (13) Fields, E. K.; Meyerson, S. *J. Am. Chem. Soc.* **1967**, 89, 3224.
- (14) Brill, T. B.; James, K. J. In *Molecular Processes in Nitroaromatic Explosives: Proof and Internal Control of the Nitro-Nitrite Rearrangement*; 11th Detonation Symposium; Office of Naval Research: Arlington, VA, 1998; p 917.
- (15) Turner, A. G.; Davis, L. P. *J. Am. Chem. Soc.* **1984**, 106, 5447.
- (16) Kaufman, J. J.; Hariharan, P. C.; Roszak, S.; Vanhemert, M. *J. Comput. Chem.* **1987**, 8, 736.
- (17) Cox, J. R.; Hillier, I. H. *Chem. Phys.* **1988**, 124, 39.
- (18) http://wulfenite.fandm.edu/Data%20Table_6.html.
- (19) Carper, W. R.; Davis, L. P.; Extine, M. W. *J. Phys. Chem. A* **1982**, 86, 459.
- (20) Golovina, N. I.; Titkov, A. N.; Raevskii, A. V.; Atovmyan, L. O. *J. Solid State Chem.* **1994**, 113, 229.
- (21) Vrcelj, R. M.; Sherwood, J. N.; Kennedy, A. R.; Gallagher, H. G.; Gelbrich, T. *Cryst. Growth Des.* **2003**, 3, 1027.
- (22) Although intermolecular reaction chemistry may not exist, the neighboring molecules create a cage effect that may alter the unimolecular chemistry conclusions. However, study of such an effect is beyond the scope of this paper.
- (23) Additional routes resulting from combining the mentioned pathways in different stages or ring fission after formation of radical species on the aromatic ring might be accessible pathways that have not been studied here. However, it should be noted that the RDS of each studied route is in most cases the initiation step; thus, the steps preceding it are less likely to contribute to the understanding of the kinetic processes leading to TNT detonation, which is the aim of this study.
- (24) Frisch, M. J.; et al. *Gaussian 03*, revision C.02; Gaussian, Inc.: Pittsburgh, PA, 2004.
- (25) Becke, A. D. *J. Chem. Phys.* **1993**, 98, 5648.
- (26) Stevens, P. J.; Devlin, F. J.; Chabalowski, C. F.; Frisch, M. J. *J. Phys. Chem.* **1994**, 98, 11623.
- (27) Dunning, T. H., Jr. *J. Chem. Phys.* **1989**, 90, 1007.
- (28) Cremer, D.; Kraka, E.; Szalay, P. G. *Chem. Phys. Lett.* **1998**, 292, 97.
- (29) Peng, C.; Ayala, P. Y.; Schlegel, H. B.; Frisch, M. J. *J. Comput. Chem.* **1996**, 17, 49.
- (30) Schlegel, H. B. *J. Comput. Chem.* **1982**, 3, 214.
- (31) Stratmann, R. E.; Burant, J. C.; Scuseria, G. E.; Frisch, M. J. *J. Chem. Phys.* **1997**, 106, 10175.
- (32) Schaftenaar, G.; Noordik, J. H. *J. Comput.-Aided Mol. Des.* **2000**, 14, 123.
- (33) He, Y. Z.; Cui, J. P.; Mallard, W. G.; Tsang, W. *J. Am. Chem. Soc.* **1988**, 110, 3754.
- (34) Guidry, R. M.; Davis, L. P. *Thermochim. Acta* **1979**, 32, 1.
- (35) Chakraborty, D.; Muller, R. P.; Dasgupta, S.; Goddard, W. A., III. *J. Phys. Chem. A* **2001**, 105, 1302.
- (36) It should be noted, however, that while the enthalpy of radical recombination/homolysis reactions may be estimated well by the calculations of reaction energetics, often there are entropic effects making this more suspect for free energy barriers. The required analysis to address this issue is beyond the scope of this paper.
- (37) Wu, C. J.; Fried, L. E. *J. Phys. Chem. A* **1997**, 101, 8675.
- (38) Chakraborty, D.; Muller, R. P.; Dasgupta, S.; Goddard, W. A. *J. Phys. Chem. A* **2000**, 104, 2261.
- (39) Willadse, P.; Zerner, B.; MacDonal, C. *J. Org. Chem.* **1973**, 38, 3411.
- (40) Shackelford, S. A.; Beckmann, J. W.; Wilkes, J. S. *J. Org. Chem.* **1977**, 42, 4201.
- (41) Gray, P.; Rathbone, P.; Williams, A. *J. Chem. Soc.* **1960**, 3932.
- (42) It should be noted that the calculated HOMO-LUMO gap for TNT is ~4.3 eV, which corresponds to ~116 kcal/mol. Accordingly, it is unlikely that TNT decomposition is promoted by excitation as the excitation energy is higher than the energy required for thermal decomposition of TNT in each of the calculated pathways.
- (43) It should be noted that all calculations were performed at atmospheric pressure. It is conceivable that under conditions of higher pressure, the temperature in which detonation begins to take place should be lower.
- (44) Strachan, A.; Kober, E. M.; van Duin, A. C. T.; Osgaard, J.; Goddard, W. A., III. *J. Chem. Phys.* **2005**, 122, 54502.
- (45) Strachan, A.; van Duin, A. C. T.; Chakraborty, D.; Dasgupta, S.; Goddard, W. A. *Phys. Rev. Lett.* **2003**, 91, 98301.